Transient current in a quantum dot asymmetrically coupled to metallic leads

2007 J. Phys.: Condens. Matter 19 376206

(http://iopscience.iop.org/0953-8984/19/37/376206)

IOP PUBLISHING JOURNAL OF PHYSICS: CONDENSED MATTER

J. Phys.: Condens. Matter **19** (2007) 376206 (9pp) doi:10.1088/0953-8984/19/37/376206

Transient current in a quantum dot asymmetrically coupled to metallic leads

A Goker[1,2], B A Friedman[3] and P Nordlander[1,2]

[1] Department of Physics, Rice Quantum Institute, Rice University, Houston, TX 77251-1892, USA
[2] Department of Electrical and Computer Engineering, Rice Quantum Institute, Rice University, Houston, TX 77251-1892, USA
[3] Department of Physics, Sam Houston State University, Huntsville, TX 77341, USA

E-mail: nordland@rice.edu

Received 17 May 2007, in final form 7 July 2007
Published 22 August 2007
Online at stacks.iop.org/JPhysCM/19/376206

Abstract

The time-dependent non-crossing approximation is used to study the transient current in a single-electron transistor attached asymmetrically to two leads following a sudden change in the energy of the dot level. We show that for asymmetric coupling, sharp features in the density of states of the leads can induce oscillations in the current through the dot. These oscillations persist to much longer timescales than the timescale for charge fluctuations. The amplitude of the oscillations increases as the temperature or source–drain bias across the dot is reduced and saturates for values below the Kondo temperature. We discuss the microscopic origin of these oscillations and comment on the possibility for their experimental detection.

(Some figures in this article are in colour only in the electronic version)

1. Introduction

Quantum effects are likely to play an increasing role in electronic devices as the physical size of their components continues to shrink. Quantum dots and qubits are examples of devices where quantum effects play a direct role in their function. In a single-electron transistor (SET), i.e. a quantum dot coupled to two metallic leads, the conductance can be drastically enhanced by the Kondo effect, which can occur when the quantum dot is populated by an odd number of electrons [1–8]. The Kondo effect is a quantum-coherent many-body state in which a spin singlet state is formed between the unpaired localized electron and delocalized electrons at the Fermi energy at low temperatures [9].

An important issue for the function of any electronic device is how fast it can respond to time-dependent perturbations and bias [10, 11]. Several studies of the time-dependent response of symmetrically coupled SET have been performed using a variety of methods [12–21]. In the case of a sudden switching of the dot level, the transient current has been found to exhibit

several distinct timescales [22–25]. The fastest timescale is associated with charge relaxation and the other much slower timescales are associated with the formation of a Kondo state, i.e. spin dynamics. The detailed evolution of the instantaneous currents following a sudden change of the dot level has been shown to depend sensitively on external parameters such as source–drain bias, external temperature, dot–lead coupling and position of the dot level. These above-mentioned time-dependent studies have all been concerned with quantum dots which are symmetrically coupled to their leads. While the effect of asymmetric coupling on the steady-state conductance of an SET has been studied both theoretically and experimentally [26, 27], to our knowledge, the transient transport properties of an asymmetrically coupled dot in the Kondo regime have not been investigated previously.

In this paper, we use a recently developed multi-scale many-body transport method to study the effect of asymmetric dot–lead coupling on the transient transport in a quantum dot [28]. We show that for a quantum dot asymmetrically coupled to two leads with sharp features in their density of states (DOS), the current can display sinusoidal modulations for timescales well beyond the fast charge relaxation timescale. The frequency of these sinusoidal modulations is given by the energy difference between the Kondo resonance and the DOS feature. The amplitude of the oscillations is found to increase with decreasing temperature and source–drain bias and saturate for temperatures below the Kondo scale. We attribute this phenomenon to an interference effect between the Kondo resonance at the Fermi level of the leads and the conduction electrons around the DOS feature. The magnitude of the oscillations depends sensitively on the structure of the DOS feature of the leads. We show that these oscillations can also occur for leads with a smooth DOS but with finite bandwidth.

2. Time-dependent current in infinite-U Anderson model

The SET is modeled as a single spin-degenerate level of energy $\varepsilon_{\rm dot}$ coupled to leads through tunnel barriers,

$$H(t) = \sum_{\sigma} \varepsilon_{\rm dot}(t) n_\sigma + \sum_{k\alpha\sigma} \varepsilon_k n_{k\alpha\sigma} + \tfrac{1}{2} \sum U n_\sigma n_{\sigma'} + \sum_{k\alpha\sigma} \left[V_\alpha(\varepsilon_{k\alpha}) c^\dagger_{k\alpha\sigma} c_\sigma + \text{h.c.} \right], \tag{1}$$

where $c^\dagger_\sigma$ (c_σ) and $c^\dagger_{k\alpha\sigma}$ ($c_{k\alpha\sigma}$) with $\alpha = \text{L, R}$ create (annihilate) an electron of spin σ in the dot level and in the left (L) and right (R) leads, respectively. The n_σ and $n_{k\alpha\sigma}$ are the corresponding number operators and V_α are the hopping amplitudes for the left and right leads. The Coulomb repulsion energy U is assumed to be sufficiently large that double occupancy of the dot level is prohibited. In the following, we will use atomic units with $\hbar = k_{\rm B} = e = 1$.

To deal with large Coulomb correlation, we use the auxiliary boson method for the Anderson Hamiltonian. Briefly, the ordinary electron operators on the site are decomposed into a massless boson operator and a pseudofermion operator as

$$c_\sigma = b^\dagger f_\sigma, \tag{2}$$

with the constraint that the number of massless 'slave' bosons plus the number of pseudofermions

$$Q = b^\dagger b + \sum_\sigma f^\dagger_\sigma f_\sigma \tag{3}$$

must be equal to unity. Self-energies for the pseudofermion and massless 'slave' boson are then projected onto the physically relevant $Q = 1$ subspace.

The Green's functions of the dot levels are calculated using the non-crossing approximation (NCA) by numerical integration on a multi-scale time grid [28]. When the

dot level $\varepsilon_{\rm dot}$ lies well below the Fermi level $\varepsilon_{\rm F}$, the spectral function of the dot (local density of states) exhibits two features: a broad Fano-like resonance of full-width

$$\Gamma_{\rm tot}(\varepsilon) = 2\pi \sum_k (|V_{\rm L}(\varepsilon_k)|^2 + |V_{\rm R}(\varepsilon_k)|^2)\delta(\varepsilon - \varepsilon_k) \tag{4}$$

around the dot level, and a sharp temperature-sensitive resonance at the Fermi level (the Kondo peak), characterized by a low energy scale $T_{\rm K}$ (the Kondo temperature)

$$T_{\rm K} \propto \left(\frac{D\Gamma_{\rm tot}}{4}\right)^{\frac{1}{2}} \exp\left(-\frac{\pi|\varepsilon_{\rm dot}|}{\Gamma_{\rm tot}}\right), \tag{5}$$

where D is a high-energy cutoff equal to half the bandwidth of the conduction electrons and $\Gamma_{\rm tot}$ corresponds to the value of $\Gamma_{\rm tot}(\varepsilon)$ at $\varepsilon = \varepsilon_{\rm F}$. All energy units in this paper will be given in terms of $\Gamma_{\rm tot}$.

The current flowing through the SET can be calculated as the difference between the currents from the left and right leads as

$$I(t) = I_{\rm L}(t) - I_{\rm R}(t). \tag{6}$$

The most general expression for the net current flowing from the left(right) lead is given by [29]

$$I_{\rm L(R)}(t) = -2\,{\rm Im}\Bigg(\int_{-\infty}^{t} {\rm d}t_1 \int \frac{{\rm d}\varepsilon}{2\pi} {\rm e}^{-{\rm i}\varepsilon(t_1-t)}\Gamma_{\rm L(R)}(\varepsilon) \times {\rm e}^{{\rm i}\int_{t_1}^{t} {\rm d}\tau\,\Delta_{\rm L(R)}(\tau)}[G^{<}(t,t_1) + f_{\rm L(R)}(\varepsilon)G^{\rm R}(t,t_1)]\Bigg), \tag{7}$$

where the coupling functions $\Gamma_{\rm L(R)}$

$$\Gamma_{\rm L(R)}(\varepsilon) = 2\pi\rho_{\rm L(R)}(\varepsilon)V_{\rm L(R)}(\varepsilon)V^{*}_{\rm L(R)}(\varepsilon), \tag{8}$$

depend on the DOS of the leads $\rho_{\rm L(R)}(\varepsilon)$ and the hopping matrix elements in equation (1). The quantity $\Delta_{\rm L(R)}$ represents the time dependence of the single-particle energies in the left and right leads. In this paper, we consider the case of a small constant bias across the leads and no explicit time and energy dependence of the hopping matrix elements, therefore $V_{\rm L(R)}(\varepsilon) = V_{\rm L(R)}(\varepsilon_{\rm f})$. We further make the assumption that the DOS of the leads are the same, i.e. $\rho_{\rm L(R)}(\varepsilon) = \rho(\varepsilon)$. Thus the coupling functions can be parameterized as,

$$\Gamma_{\rm L(R)}(\varepsilon) = \bar{\Gamma}_{\rm L(R)}\rho(\varepsilon), \tag{9}$$

where $\bar{\Gamma}_{\rm L(R)}$ are constants given by $\bar{\Gamma}_{\rm L(R)} = 2\pi|V_{\rm L(R)}(\varepsilon_{\rm f})|^2$ and they determine the asymmetry of the couplings. In terms of these constants, $\Gamma_{\rm tot} = (\bar{\Gamma}_{\rm L} + \bar{\Gamma}_{\rm R})\rho(\varepsilon_{\rm f})$.

In figure 1 we show the functions $\rho(\varepsilon)$ that will be used to model the leads. The Lorentzians used in figures 1(c) and (d) to model sharp DOS features have a width equal to $0.002\ \Gamma_{\rm tot}$. The DOS function $\rho(\varepsilon)$ has been normalized for all cases such that the bands contain the same number of electrons. The bandwidth of the leads is assumed to be $2D$ with the Fermi energy at $\varepsilon = 0$.

The expression for the current can then be written as

$$I(t) = -2\bar{\Gamma}_{\rm L}\,{\rm Im}\Bigg(\int_{-\infty}^{t} {\rm d}t_1 (G^{<}(t,t_1)h(t-t_1) + G^{\rm R}(t,t_1)f_{\rm L}(t-t_1))\Bigg) + 2\bar{\Gamma}_{\rm R}\,{\rm Im}\Bigg(\int_{-\infty}^{t} {\rm d}t_1 (G^{<}(t,t_1)h(t-t_1) + G^{\rm R}(t,t_1)f_{\rm R}(t-t_1))\Bigg), \tag{10}$$

where

$$h(t-t_1) = \int_{-D}^{D} \frac{{\rm d}\varepsilon}{2\pi}\rho(\varepsilon){\rm e}^{{\rm i}\varepsilon(t-t_1)}, \tag{11}$$

$$f_{\rm L}(t-t_1) = \int_{-D}^{D} \frac{{\rm d}\varepsilon}{2\pi}\rho(\varepsilon)\frac{{\rm e}^{{\rm i}\varepsilon(t-t_1)}}{1+{\rm e}^{\beta[\varepsilon-\frac{V}{2}]}}, \tag{12}$$

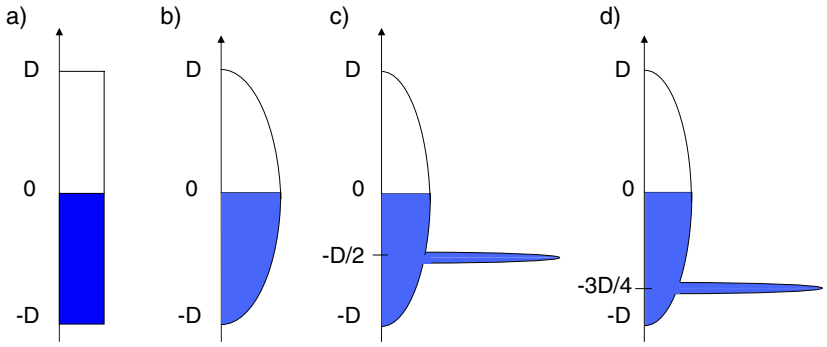

Figure 1. This figure shows the functions $\rho(\varepsilon)$ used to model the leads. Panel (a) corresponds to a rectangular band, (b) to a parabolic band, and (c) and (d) to parabolic bands with a Lorentzian feature located at $\varepsilon = -D/2$ and $-3D/4$, respectively.

and

$$f_{\mathrm{R}}(t-t_1) = \int_{-D}^{D} \frac{\mathrm{d}\varepsilon}{2\pi}\rho(\varepsilon)\frac{\mathrm{e}^{\mathrm{i}\varepsilon(t-t_1)}}{1+\mathrm{e}^{\beta[\varepsilon+\frac{V}{2}]}}. \tag{13}$$

In these expressions, V represents the source–drain bias.

The physical Green's functions in equation (10) can be expressed in terms of the pseudofermion and slave boson Green's functions using a projection approach discussed previously [30]. The final expression for the current is

$$\begin{aligned} I(t) = -2\bar{\Gamma}_{\mathrm{L}}\,\mathrm{Im}\Bigg(\int_{-\infty}^{t}\mathrm{d}t_1 (G^{<}_{\mathrm{pseudo}}(t,t_1)B^{\mathrm{R}}(t_1,t)h(t-t_1)\Bigg) \\ -\mathrm{i}((G^{\mathrm{R}}_{\mathrm{pseudo}}(t,t_1)B^{<}(t_1,t)+G^{<}_{\mathrm{pseudo}}(t,t_1)B^{\mathrm{R}}(t_1,t))\,f_{\mathrm{L}}(t-t_1))) \\ +2\bar{\Gamma}_{\mathrm{R}}\,\mathrm{Im}\Bigg(\int_{-\infty}^{t}\mathrm{d}t_1 (G^{<}_{\mathrm{pseudo}}(t,t_1)B^{\mathrm{R}}(t_1,t)h(t-t_1)\Bigg) \\ -\mathrm{i}((G^{\mathrm{R}}_{\mathrm{pseudo}}(t,t_1)B^{<}(t_1,t)+G^{<}_{\mathrm{pseudo}}(t,t_1)B^{\mathrm{R}}(t_1,t))\,f_{\mathrm{R}}(t-t_1))). \end{aligned} \tag{14}$$

This is the main result of this section and will be used in the calculations presented below.

3. Results

In this section we will analyze the instantaneous current following a sudden change of the dot level from a position at $\varepsilon_1 = 5\Gamma_{\mathrm{tot}}$ below the Fermi level where, for the present finite temperatures, the Kondo effect will be absent to a position at $\varepsilon_2 = 2\Gamma_{\mathrm{tot}}$ closer to the Fermi energy where the Kondo effect will be present. For a parabolic DOS function (figure 1(b)) with $D = 9\Gamma_{\mathrm{tot}}$, the Kondo temperature in the final state is approximately $T_{\mathrm{K}} = 0.0016\Gamma_{\mathrm{tot}}$.

We begin our analysis by investigating the effect of asymmetric coupling to the leads. We define the asymmetry factor as the the ratio $\bar{\Gamma}_{\mathrm{L}}/\bar{\Gamma}_{\mathrm{tot}}$, where $\bar{\Gamma}_{\mathrm{tot}} = \bar{\Gamma}_{\mathrm{L}} + \bar{\Gamma}_{\mathrm{R}}$. In figure 2, the instantaneous conductance, $G = I(t)/V$, is plotted as a function of time after the dot level is switched for various asymmetry factors with small bias. The final steady-state conductances are in perfect agreement with previous theoretical results [31]. The transient short timescale associated with Γ_{tot} shown in figure 2(a) is due to the formation of the broad Fano-like resonance at ε_2. The transient increase in the instantaneous current is due to the charging of the dot. The steady-state current is determined by the asymmetry factor. For an asymmetry factor of 1 where the steady-state current is zero, we have verified the accuracy of our numerical

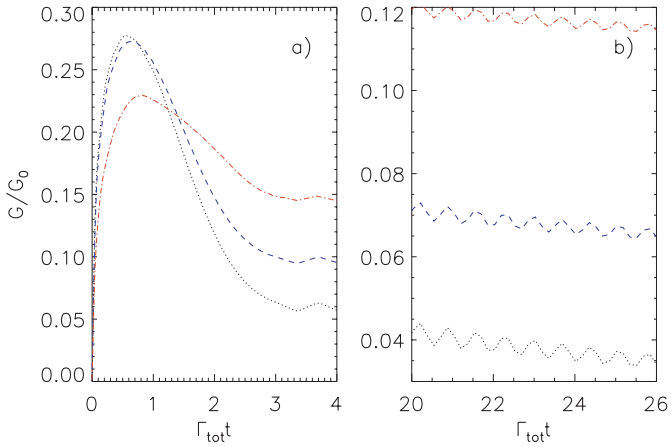

Figure 2. Black (dotted), blue (dashed) and red (dot–dashed) curves in panel (a) show the instantaneous conductance versus time for rectangular DOS in figure 1(a) immediately after the dot level is switched to its final position for asymmetry factors of 0.95, 0.9 and 0.85, respectively. $\Gamma_{\rm tot}$ is fixed with $D = 9\Gamma_{\rm tot}$ at $T = 0.0093\Gamma_{\rm tot}$ and $V = T_{\rm K}$. The beginning of the oscillations is clearly visible in this panel. Black (dotted), blue (dashed) and red (dot–dashed) curves in panel (b) are the continuation of those in the first panel in the long timescale for the same parameters.

approach by showing that the integrated current is equal to the change in the charge of the dot level.

Figure 2(b) shows the instantaneous conductances for larger times on a magnified scale. It is clear from this panel that the current exhibits sinusoidal modulations at timescales well beyond $\Gamma_{\rm L}$ or $\Gamma_{\rm R}$. As we reduce the asymmetry factor, the amplitude of these sinusoidal modulations starts decreasing and eventually disappears for symmetric coupling. The frequency of the conductance oscillations is equal to the bandwidth D of the leads. External parameters such as the energy or width of the dot level, asymmetry factor, and ambient temperature and source–drain bias only influence the amplitude of the oscillations.

In figure 3 we show the effect of the the DOS function of the leads, $\rho(\epsilon)$, on the conductance oscillations. The oscillations do not look like perfectly sinusoidal functions because of our use of a finite time step in the numerical solution of the Dyson equations. However, the results are fully converged and for finer time steps we recover almost perfectly sinusoidal oscillations. Figure 3 reveals that the DOS can have a pronounced effect on the conductance oscillations. The largest oscillations occur for a DOS with a peak feature as in figures 1(c) and (d). For a parabolic DOS function (figure 1(b)), conductance oscillations are still present but not discernible on the scale of the figure. The frequency of the current oscillations is equal to the energy difference between the Fermi level of the leads and the feature in the DOS function. For the rectangular and parabolic DOS function (figures 1(a) and (b)) where the DOS feature is the band cut-off, the period is equal to $1/D = 1/9$ and, for the DOS functions depicted in figures 1(c) and (d) where the DOS feature is the narrow Lorentzian peak, the periods are $2/D$ and $4/3D$, respectively.

We have also investigated other shapes of DOS functions. For instance, for a triangular DOS, $\rho(\varepsilon) = 2(1 + \varepsilon/D)$, the conductance displays oscillations whose frequency is equal to D, very similar to what was obtained for the parabolic DOS in figure 1(b). For two sharp features at different energies D_1 and D_2 in the DOS, we obtain conductance modulations of frequencies proportional to $(D_1 + D_2)$ and $(D_1 - D_2)$.

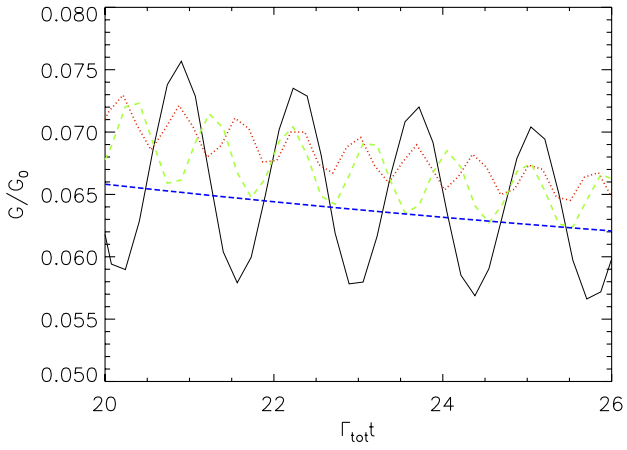

Figure 3. Effect of the DOS function on the instantaneous conductance. Red (dotted), dark blue (dot–dashed), black (solid) and green (dashed) curves display the instantaneous conductance versus time in the long timescale for cases (a), (b), (c) and (d), respectively, in figure 1 when the source–drain bias is equal to $V = T_K$ with fixed Γ_{tot}. All curves are for an asymmetry factor of 0.9, $D = 9\Gamma_{tot}$ at $T = 0.0093\Gamma_{tot}$.

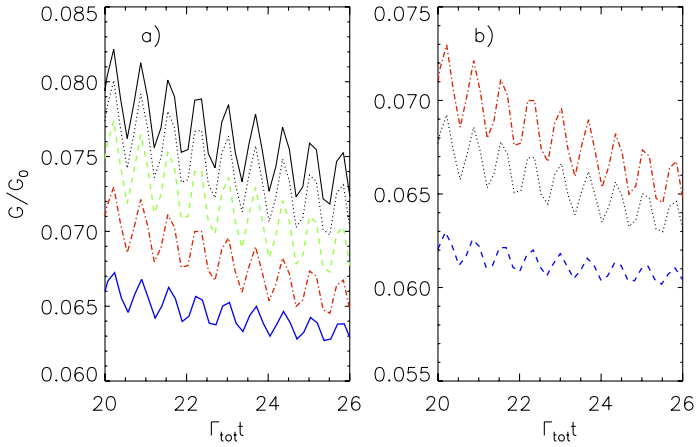

Figure 4. Panel (a) shows the instantaneous conductance for several different temperatures with asymmetry factor of 0.9, fixed Γ_{tot}, $D = 9\Gamma_{tot}$ and rectangular DOS. Dark blue (dot–dot–dashed), red (dot–dashed), green (dashed), light blue (dotted) and black (solid) curves represent the conductance at $T = 0.0186$, 0.0093, 0.0046, 0.0023, and $0.0009\Gamma_{tot}$, respectively. Red (dot–dashed), black (dotted) and dark blue (dashed) curves in panel (b) display the instantaneous conductance versus time in the long timescale for rectangular DOS when the source–drain bias is equal to $V = T_K$, $V = 5T_K$ and $V = 10T_K$, respectively, with fixed Γ_{tot} and $D = 9\Gamma_{tot}$ for an asymmetry factor of 0.9 at $T = 0.0093\Gamma_{tot}$.

Figure 4 shows the effect of temperature and source–drain bias on the conductance oscillations. The figure demonstrates that the amplitude of the oscillations decreases with temperature and bias across the dot but their frequency remain unchanged. The figure shows two important effects. First, it takes longer for the current and thus the damped oscillations to decay as the temperature or source–drain bias is reduced. Second, the amplitude of the damped oscillations increases with decreasing temperature or source–drain bias but saturates

for temperatures and bias below the Kondo temperature, which we estimate to be around $T_K = 0.0016\Gamma_{tot}$ in these systems.

4. Discussion

Our numerical calculations clearly show that the timescale for the decay of the conductance oscillations is much larger than the fast timescales set by the couplings of the dot level to the leads, Γ_L or Γ_R. The timescale does not depend on the width or shape of the DOS feature in the leads. It appears that the timescale is related to the Kondo resonance. When the Kondo resonance is fully formed at times around $1/T_K$, the oscillations disappears.

Further support for the role of Kondo physics in these conductance oscillations comes from the observation of a saturation of their amplitude for temperatures and source–drain bias below the Kondo temperature (figure 4). The effect of temperature and source–drain bias on the Kondo resonance in an SET was recently investigated in detail [23]. For values smaller than the Kondo temperature, the Kondo resonance is fully formed just above the Fermi level. Increasing the temperature above T_K broadens and reduces the magnitude of the resonance. Increasing the source–drain bias results in the formation of a split Kondo resonance with strongly reduced intensities. For temperatures or source–drain bias well above the Kondo temperature, the Kondo resonance is completely suppressed. Since the frequency of the oscillations is determined by the energy difference between the Fermi level and the DOS feature, we believe that the oscillations reflect an interference process between the conduction electrons associated with the Kondo resonance and the conduction electrons associated with the DOS feature. In order to substantiate this explanation, we used a simple analytical non-interacting Anderson model to calculate the instantaneous conductance following the sudden switching of a dot level of width Γ_{eff} equal to that of the final Kondo resonance in the interacting model. This effective resonance was switched to a position just above the Fermi level of the leads. These calculations were performed numerically for both the parabolic and rectangular DOS functions shown in figures 1(a) and (b). The instantaneous conductance was found to display the same conductance oscillations with frequencies determined by the bandwidth D as in the original interacting model. The oscillations are found to decay over a long timescale determined by Γ_{eff}.

While the Kondo temperature depends only on the total coupling to the leads Γ_{tot}, the total current depends on the asymmetry factor. The reason why the conductance oscillations only show up for asymmetric couplings is that the total current through the dot is the difference between the currents from the left and right leads, equation (6). The interference effect shows up both in the right and the left currents. For symmetric coupling, the current oscillations from the right and left leads are out of phase, resulting in a cancellation of the oscillations in the total current. For asymmetric coupling the left and right current oscillations do not cancel, resulting in the observed conductance oscillations. This result has also been verified numerically for the non-interacting model described in the preceding paragraph.

For dots coupled to leads with very weak DOS features, the conductance oscillations will be very small. In figure 5 we show the time derivative of the instantaneous current for leads with a parabolic DOS function (figure 1(b)) for three different values of the bandwidth D. The conductance oscillations here result from the interference of the Kondo resonance in the final state and the weak discontinuity in the DOS at the lower band edge of the leads. The figure clearly demonstrates oscillations of the instantaneous currents with a frequency equal to D in the long timescale.

The experimental study of the conductance oscillations could possibly be made using previously suggested techniques, i.e. by measuring the total charge transport as a function

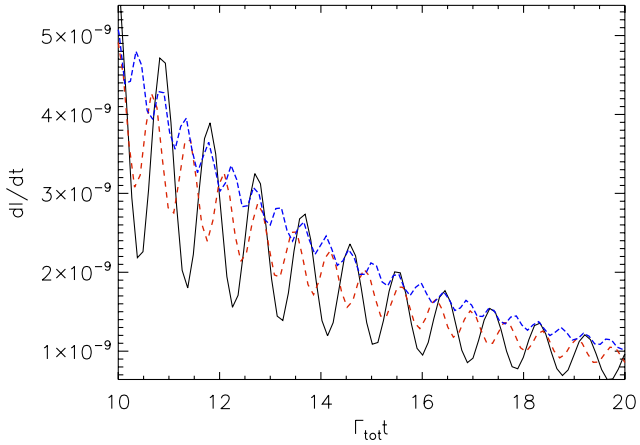

Figure 5. Time derivative of the instantaneous current in the long timescale for parabolic DOS (figure 1(b)). Black (solid), red (dashed) and dark blue (dot–dashed) curves correspond to $D = 6.75\Gamma_{\rm tot}$, $D = 9\Gamma_{\rm tot}$ and $D = 13.5\Gamma_{\rm tot}$ for an asymmetry factor of 1.0 at $T = 0.0093\Gamma_{\rm tot}$.

of pulse duration [15]. For a bandwidth of $D = 1$ eV, the oscillation period will be of the order of 10^{-14} s. Since the current oscillates, electromagnetic radiation will be emitted at a rate proportional to $[\frac{dI(t)}{dt}]^2$. For a suitably designed system it may be possible to detect the emitted light. For $D = 1$ eV the emission would occur in the infrared at a photon energy of 0.1 eV.

5. Conclusion

In this paper, we employed the time-dependent non-crossing approximation to analyze the transient current in a single-electron transistor in the Kondo regime asymmetrically coupled to two metallic leads with features in their DOS. We show that, for asymmetric coupling, the conductance can exhibit oscillations which persist for times much longer than the timescale for charge relaxation. The origin of these oscillations is an interference between the conduction electrons associated with the Kondo resonance and those associated with the DOS feature. The amplitude of the oscillations are found to depend strongly on the temperature and source–drain bias when these exceed the Kondo temperature. We hope that our predictions will motivate further theoretical and experimental studies.

Acknowledgments

We thank Professor Hong Guo for communication regarding relevant work [32]. This work was supported by the Welch Foundation under grant C-1222.

References

[1] Ng T K and Lee P A 1988 *Phys. Rev. Lett.* **61** 1768
[2] Pustilnik M and Glazman L 2004 *J. Phys.: Condens. Matter* **16** R513–37
[3] Giuliano D, Naddeo A and Tagliacozzo A 2004 *J. Phys.: Condens. Matter* **16** S1453–83
[4] Goldhaber-Gordon D, Shtrikman H, Mahalu D, Abusch-Magder D, Meirav U and Kastner M A 1998 *Nature* **391** 156–9
[5] Cronenwett S M, Osterkamp T H and Kouwenhoven L P 1998 *Science* **281** 540–4

[6] Hewson A C, Bauer J and Oguri A 2005 *J. Phys.: Condens. Matter* **17** 5413–22
[7] Jiang Z T and Sun Q F 2007 *J. Phys.: Condens. Matter* **19** 156213
[8] Galperin M, Ratner M A and Nitzan A 2007 *J. Phys.: Condens. Matter* **19** 103201
[9] Kondo J 1964 *Prog. Theor. Phys.* **32** 37
[10] Elzerman J M, Hanson R, van Beveren L H W, Witkamp B, Vandersypen L M K and Kouwenhoven L P 2004 *Nature* **430** 431–4
[11] Xing Y, Sun Q F and Wang J 2007 *Phys. Rev.* B **75** 125308
[12] Hettler M H and Schoeller H 1995 *Phys. Rev. Lett.* **74** 4907
[13] Schiller A and Hershfield S 1996 *Phys. Rev. Lett.* **77** 1821
[14] Goldin Y and Avishai Y 1998 *Phys. Rev. Lett.* **81** 5394
[15] Nordlander P, Pustilnik M, Meir Y, Wingreen N S and Langreth D C 1999 *Phys. Rev. Lett.* **83** 808–11
[16] Kaminsky A, Nazarov Y V and Glazman L I 1999 *Phys. Rev. Lett.* **83** 384
[17] Schiller A and Herschfield S 2000 *Phys. Rev.* B **62** R16271–4
[18] Kogan A, Amasha S and Kastner M A 2004 *Science* **304** 1293
[19] Lobaskin D and Kehrein S 2005 *Phys. Rev.* B **71** 193303
[20] Monreal R C and Flores F 2005 *Phys. Rev.* B **72** 195105
[21] Galperin M, Nitzan A and Ratner M A 2007 *Phys. Rev.* B 035301
[22] Merino J and Marston J B 2004 *Phys. Rev.* B **69** 115304
[23] Plihal M, Langreth D C and Nordlander P 2005 *Phys. Rev.* B **71** 165321
[24] Anders F B and Schiller A 2005 *Phys. Rev. Lett.* **95** 196801
[25] Anders F B and Schiller A 2006 *Phys. Rev.* B **74** 245113
[26] Krawiec M and Wysokinski K I 2002 *Phys. Rev.* B **66** 165408
[27] Quirion Q, Weiss J and v Klitzing K 2006 *Eur. Phys. J.* B **51** 413–9
[28] Izmaylov A F, Goker A, Friedman B A and Nordlander P 2006 *J. Phys.: Condens. Matter* **18** 8995–9006
[29] Jauho A P, Wingreen N S and Meir Y 1994 *Phys. Rev.* B **50** 5528
[30] Shao H X, Langreth D C and Nordlander P 1994 *Phys. Rev.* B **49** 13929–47
[31] Wingreen N S and Meir Y 1994 *Phys. Rev.* B **49** 11040
[32] Maciejko J, Wang J and Guo H 2006 *Phys. Rev.* B **74** 085324